fibrils form such a group. Since the PFM technique is sensitive mainly to the surface (few nanometers to few tens of nanometers, depending on the contact mechanics), we extrapolate that the nano-domains have a similar size in the depth of fascia.

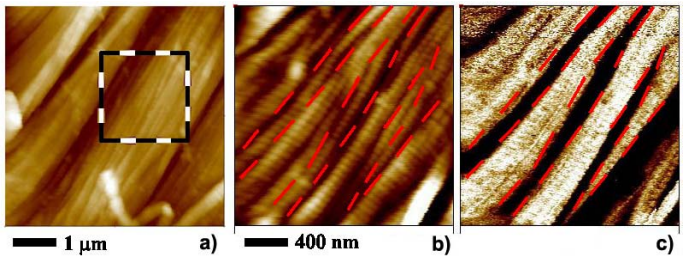

Fig. 5. Piezoresponse force microscopy experiment on fascia. a) sample topography, 5μm scan, (b) topography, zoom of (a), and (c) piezoresponse image [of the same area as in (b)] showing the orientation of the piezoelectric tensor. The piezoelectric response in fascia has either a positive or negative value (white or a dark contrast).

To further confirm the structural origin of noncentrosymmetricity in fascia, we analyzed the piezoelectric response of one single isolated fibril (Fig. 6, see next page) in order to clarify the imaging contrast observed in the PFM image of Fig. 5(c). For this purpose, we recorded several PFM images of the same location at different orientations between the cantilever of the collagen fibril, by rotating the sample under the probing tip. In Fig. 6, we show the dependence of the PFM signal on the angle between cantilever and the fibril axis. The PFM signal could be fit with a cosine function, implying that the piezoelectric response is primarily a shear displacement along the fibril axis. The insets of Fig. 6 show two of the images used to calculate the points of the graph. The results presented in this last figure are showing that isolated collagen fibrils are noncentrosymmetric (piezoelectric) and that the sign of the second order nonlinear optical susceptibility is maintained along the fibrillar axis over several microns. Additionally, a careful analysis of the signal strength generated by isolated fibrils, as well as comparison with results on collagen from bovine [42] have shown that the signal is uniform across the fibril diameter, suggesting that the the whole volume of the fibril is piezoelectric and not only the surface. Indeed, as Kholkin et *al.* observed in peptide nanotubes, the PFM signal is maximum at the edge (corresponding to the tube wall) and

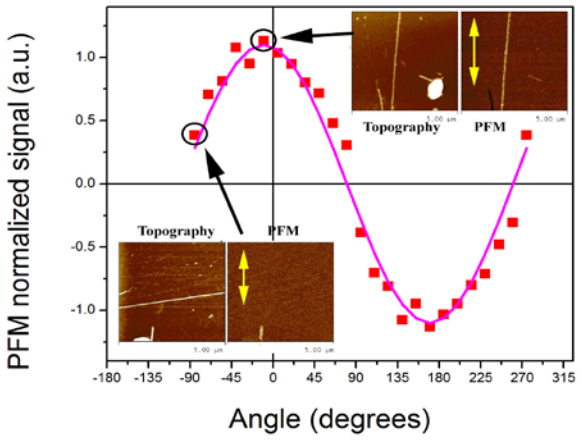

Fig. 6. The dependence of the PFM signal (in-plane measurements) on the angle between the cantilever and the collagen fibril axis, averaged over a 5μm of fibril length. The single collagen fibril was rotated in steps of 15 degrees. The insets illustrate two of the image sets (each composed of topography at left and PFM image at right, 5μm scans) used to construct the graph. The yellow arrows in the PFM images illustrate the detection direction.

#136355- $15.00USD Received11 Oct 2010;revised16 Nov 2010;accepted29 Nov 2010;published1 Dec 2010

clearly decreases at the center (corresponding to on the crest of the tube) when the tube wall is thin [43]. A non-homogeneous distribution (such as "core-shell") of piezoelectric material within the fibril would thus imply a weaker PFM response of the thin piezoelectric shell in the central region. Therefore, the high-resolution PFM results support one of the models proposed by Strupler and Schanne-Klein to simulate SHG from tissues rich in collagen type I proteins, where the $\chi^{(2)}$ scatterers are distributed uniformly within the volume of the fibrils represented as cylinders, and the phase of $\chi^{(2)}$ is allowed to flip by 180 degrees from one fibril to another [37].

4. Conclusion

In this paper, we used second harmonic generation and piezoresponse force microscopy techniques to image noncentrosymmetric structures in fascia. The measurements performed with SHG microscopy reveal that the distribution of $\chi^{(2)}$ scatterers is heterogeneous on a spatial scale inferior to the resolution provided by the nonlinear optical microscope (sub-micron). Comparing forward and backward images indicates that the continuous patterns observed in the direction of laser propagation are not fibers but regions where the phase matching condition is better satisfied. In the backward direction, the SHG signal is nearly uniform across the collagen sheets of fascia revealing that noncentrosymmetric structures are present everywhere within the spatial resolution provided by the nonlinear optical microscope. Furthermore, the large modulations observed in the forward SHG images suggest that the nanoscale architecture of $\chi^{(2)}$ scatterers changes rapidly in the transverse direction to the fibrillar axis. Measurements of the forward signal as a function of the numerical aperture of collection lead to the same conclusion but along the direction of laser propagation.

Using piezoresponse force microscopy, a scanning probe technique also sensitive to the presence of noncentrosymmetric structures and providing sub-10 nm spatial resolution, we demonstrated that an individual collagen fibril has a noncentrosymmetric structural organization, with an anisotropic axis maintained along the fibrillar axis. Fibrils are found to be organized into nano-domains where the anisotropic axis is uniformly directed along the fibrillar axis. Across the collagen sheets of fascia, in the direction transverse to the fibrillar axis, the phase of the second order nonlinear susceptibility is changing by 180 degrees between adjacent nano-domains. We extrapolate that they have a similar size in the depth of fascia. The experimental results presented in this paper confirm the essence of one model used by Strupler and Schanne-Klein to simulate SHG from tendon, namely a uniform distribution of scatterers throughout the whole fibril volume with random 180° polarization flips [30], a tissue rich in collagen type I proteins like fascia. The complex nanoscale architecture of $\chi^{(2)}$ scatterers governs the phase matching condition and allows forward and backward SHG in the bulk of collagen tissues as opposed to SHG in the bulk of homogenous crystal such as quartz. An analogy with periodically poled crystals used for efficient SHG conversion can be drawn, but in the case of tissues rich in collagen type I proteins, the periodicity is not well defined and changes across the collagen sheets. Henceforth, describing fascia as a nanometric randomly poled crystal would be more accurate.

Acknowledgments

The authors acknowledge the financial support from INRS, the Canada Foundation for Innovation (CFI), the Natural Sciences and Engineering Research Council of Canada (NSERC), Le Fonds Québécois de la Recherche sur la Nature et les Technologies (FQRNT), Le Ministère du Développement Économique, Innovation et Exportation (MDEIE) du Québec, the Canadian Institutes for Health Research (CIHR), and the Canadian Institute for Photonic Innovations (CIPI).

#136355 - $15.00 USD Received 11 Oct 2010; revised 16 Nov 2010; accepted 29 Nov 2010; published 1 Dec 2010
(C) 2011 OSA